March - April 2020
ISSN: 0193-4120 Page No. 12495 - 12505

Auto Segmentation of Retinal Blood Vessel Image using 2-D Gaussian Filter and Its First and Second Order Derivative

Manjunath V Gudur[1], Shreeshayana R[2], Dr. Naveen K B[3], Mr. Naveen H[4],
CMR Institute of Technology, Bangaluru[1]
ATME College of Engineering, Mysuru[2]
BGS Institute of Technology, Mandya[3]
Assistant professor NHCE, Bangalore[4]

Article Info
Volume 83
Page Number: 12495 - 12505
Publication Issue:
March - April 2020

Article History
Article Received*: 24 July 2019*
Revised*: 12 September 2019*
Accepted*: 15 February 2020*
Publication*: 18 April 2020*

Abstract
we are presenting a novel unsupervised way of segmenting the vasculature in images of retina. This technique employs a FODOG and SODOG 2-D Gaussian filters with the modified local entropic thresholding algorithm for segmenting vasculature of retinal images. The algorithm is implemented on STARE and DRIVE datasets which are freely available. The SODOG method gives better performance on both databases in comparison with other existing techniques. On STARE and DRIVE database, it achieves average segmentation accuracy of 96.37% and 96.82% respectively. The time taken by the proposed algorithm for processing each retinal image is very less compared to other existing supervised methods. The simpleness and fast execution makes the proposed algorithm appropriate for automated analysis of retinal images thereby aids in diagnosing the diabetic retinopathy.

Keywords: *Diabetic retinopathy, Gaussian, Modified local entropy thresholding, Vessel segmentation. Retina.*

I. INTRODUCTION

Diabetic Retinopathy (DR) causes blindness in patients with diabetes. Diabetic patients are 25 times more susceptible to blindness than non-diabetic ones [1]. Reports of WHO (world-Health Organization) states global diabetic prevalence n the year 2000 was 2.8% and is estimated to become 4.4% by 2030. Diabetic patients were 171 million in the year 2000 and are estimated to reach 366 million in 2030 [2]. India is set to emerge as the diabetic capital of the world. In India there were about 31.7 million people with diabetes in the year 2000 with an estimation to reach the figure of 79.4 million in 2030. A screening procedure to detect DR in the beginning stage is getting attention of health care sector in India [1].

Patients with diabetes are more susceptible to changes in the vascular network of retina, and these structural changes of retina are termed as diabetic retinopathy. In DR, blood vessels of retina undergo a series of changes like leakages or closing of vessel [3]. The main perspective in performing automatic detection of blood vessels is to inspect and aid the physicians in diagnosing ocular diseases like arteriosclerosis, cardiovascular disease; patient screening like hypertension, diabetes etc [4]. Best remedy for eye related diseases is the detection of diseases in early stages [5]-[7].

Diabetic patients will not get any symptoms until the last stage where vision loss occurs, where the treatment is not effective. Hence, for the effective treatment, patients with diabetes should take regular screenings on yearly basis. Early detection of DR is a biggest challenge for the healthcare sector because of large group of patients in need of eye examination.Structural analysis and manual measurements of retinal vasculature suffers from human error. So, the viable solution to this problem is to use computerized analysis, which can be used effectively by non-experts to

March - April 2020
ISSN: 0193-4120 Page No. 12495 - 12505

separate out the patients without DR, thereby reducing specialist's work load.

In this paper, Gaussian based first-order and second-order derivative filters are used with modified local entropy thresholding algorithm. The method is simple and high in accuracy in segmenting the blood vessels compared with those reported in literature.Section II of the paper covers literature work on segmentation of vascular network. Section III explains about datasets used. Section IV describes the proposed algorithm used in segmenting the vascular network of retina. Section V is about results and performance evaluation of two filter based methods. Last part is about discussion followed by conclusion.

II. RELATED WORK

Retinal vessel segmentation methods available in the literature are categorized as supervised and unsupervised, where supervised require training images and unsupervised does not. Supervised methods use classifiers in order to classify pixels as vessel or background pixels. [8] Proposes K-nearest neighbor classifier method to classify pixels into vessel or non-vessels. [9] Presented supervised ridge based vessel detection method. Here 27 features were computed and are classified by using kNN classifier. [10] presented a technique in which 2D Gabor wavelet transform response taken at different scales and the inverted green channel were given as pixel feature vectors for the Gaussian mixture model Bayesian classifier. [11] Uses line detectors with pixel gray value to construct the feature vector followed by support vector machine (SVM) classifier to classify the pixels. [12] Proposed a multilayered feed forward NN scheme for segmenting retinal vasculature. Regarding unsupervised (rule based) techniques, vessel tracking approaches [13] - [19] detects vascular structure, and parameters of vessels like diameters and branching points etc.

[20] Presented a Matched filter technique of segmenting vascular network. [21] Presented a technique of segmenting the vasculature of retina by piecewise threshold probing of a matched filter, where response of filter is used for segmenting vessels. [22] Presented matched filter with entropy thresholding method for vessel segmentation. The papers [23] - [25] use mathematical morphological operators for filtering vasculature. [26] Presented a method which uses multi threshold probing for vessel segmentation. [27] Presented multiscale feature extraction and classification technique. [28] Used gradient orientation technique in order to segment the retinal vasculature . Related works shows finding the vessel location helps in decreasing false positive fractions in the detecting microaneurysm and hemorrhages. [29]-[31].

Here we have proposed an unsupervised retinal vasculature segmentation algorithm using first order and second order derivatives of Gaussian with modified local entropy thresholding algorithm. Here we have introduced two modifications to thresholding algorithm in order to improvise the performance by detecting detailed and clear vascular structure. Firstly, co-occurrence matrix is modified to enhance local entropy. Secondly, sparse foreground is considered in selecting the optimal threshold in segmenting vessel and background pixels. [35] Presents fully convolution method (FCN) with Sobel operators.The method is used in recognition of vasculature of retina in patients with cataract.

III. MATERIALS

Here we used DRIVE [32] and STARE [33] datasets for study. DRIVE dataset has 20 retinal images (in that 7 has pathology) captured with a Canon camera. The images are with size 768×584 pixels and available in TIFF format. The STARE dataset, has 20 retinal images (in that 10 with pathology) captured with a fundus camera. The images are with size 700 ×605 pixels and available in PPM format. Two databases comprises of manual segmentations of blood vessels by two different specialists. Ground truth images from first specialist are used in evaluating the performance of the proposed method.

IV. PROPOSED VESSEL SEGMENTATION ALGORITHM

The proposed retinal vasculature segmentation technique consists of four steps: 1) preprocessing that includes the extraction of green band image from input RGB image of retina. 2) filtering by derivatives of Gaussian, 3) segmentation by modified local entropy thresholding algorithm to classify vessels and background in the filtered image. 4) Post processing by length filtering to remove misclassified pixels.

March - April 2020
ISSN: 0193-4120 Page No. 12495 - 12505

RGB retinal image is separated into red, blue and green band image. The green band image is used as input to filter because it presents better vessel-background contrast [24] compared with other red and blue bands. Fig. 1(a) and Fig 1(b) shows the input RGB image of retina from STARE dataset output of preprocessing that is the green band image respectively.The gray level intensity profiles of the cross section of blood vessels in preprocessed images of retina can be modeled by a Gaussian shaped curve [21] hence Gaussian filter is designed to enhance the vessels.

The zero-mean 2D Gaussian is expressed as:

$$G(x,y) = -e^{-\frac{x^2+y^2}{2\sigma^2}} \qquad \text{for } y \le \frac{L}{2} \tag{1}$$

With normalizing factor equation-(1) is written as

$$G(x,y) = -\frac{1}{2\pi\sigma^2} e^{-\frac{x^2+y^2}{2\sigma^2}} \qquad \text{for } y \le \frac{L}{2} \tag{2}$$

Figure 1 Illustration of Pre-processing: (a) Retinal image from STARE database. (b) Extracted green band image of the retinal image.

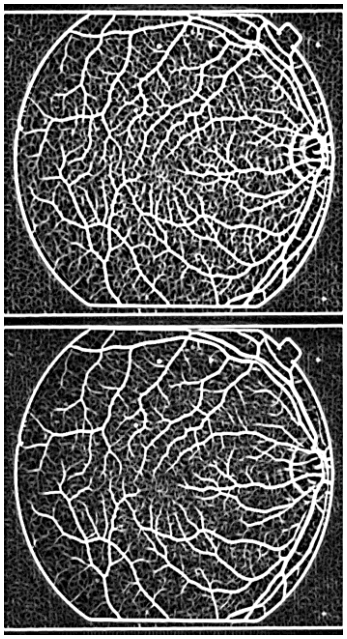

Figure 2. Illustration of Gaussian filtered images: (a) Filtered image from FODOG b) Filtered image from SODOG

A. FODOG

First order derivative of a 2D Gaussian can be obtained from equation –(2) as follows

$$G'(x,y) = \frac{(x^2+y^2)}{\sigma^2} e^{-\frac{x^2+y^2}{2\sigma^2}} \tag{3}$$

$$\text{for } y \le \frac{L}{2}$$

Where, "σ" indicates filter scale; "*L"* is vessel length for which it is assumed to have fixed orientation. And hence vessel direction is assumed to be aligned along the y-axis.A group of 12, 15x16 pixel filter kernels are designed and convolved with the fundus image. And in the resultant set of images highest magnitude at each pixel is selected as illustrated in Fig. 2(a).

B. SODOG

Second order derivative of a Gaussian is obtained as

$$G''(x,y) = -\frac{1}{\sigma^2}\left(\frac{x^2+y^2}{\sigma^2} - 1\right) e^{-\frac{x^2+y^2}{2\sigma^2}} \tag{4}$$

$$\text{for } y \le \frac{L}{2}$$

March - April 2020
ISSN: 0193-4120 Page No. 12495 - 12505

After introducing a normalizing multiplicative, we get SODOG mask as follows

$$G''(x,y)=\frac{1}{\pi\sigma^4}\left(1-\frac{x^2+y^2}{2\sigma^2}\right)e^{-\frac{x^2+y^2}{2\sigma^2}} \quad (5)$$

for $y \le \frac{L}{2}$

The parameters are same as discussed in FODOG. Here we used eight 15x16 pixel filter kernels for convolving with fundus image. And in the resultant set of images highest magnitude at each pixel is selected, Fig. 2(b) represents filter response image.

C. *Modified Local Entropy Thresholding*

Here performance of the method is improved by introducing two alterations to existing co-occurrence matrix.

Cooccurrence matrix of the image I is a $M \times N$ dimensional matrix $R = [r_{lk}]_{MxN}$ which tells about the intensity transition between neighbourhood pixels. The existing matrix [22] is asymmetric which considered horizontal right and vertical lower intensity transitions between adjacent pixels. Here the matrix is manipulated asymmetric by taking horizontal right and diagonal intensity transition between adjacent pixels. Hence, r_{ld} is represented by following equation:

$$r_{ld} = \sum_{i=1}^{M}\sum_{j=1}^{N}\delta \quad (6)$$

Where, $\delta = 1$ if $I(i,j) = l$

$I(i, j+1) = k$
$I(i+1, j+1) = d$ and

δ =0 otherwise

For every pixel *(i, j)* in an image *I*

l = I (i, j);

k = I (i, j + 1);

d = I (i+ 1, j + 1);

$r_{lk} = r_{ld} + 1$;

End

Intensity transitions between adjacent pixels with gray levels l and k is expressed with probability of the co-occurrence P_{lk} as shown,

$$P_{lk} = \frac{r_{lk}}{\sum_l \sum_k r_{lk}} \quad (7)$$

Considering t, $0 \le t \le S-1$, as initial threshold value co-occurrence matrix is divided into 4 parts, namely W, X, Y, and Z as shown in Fig. 3.

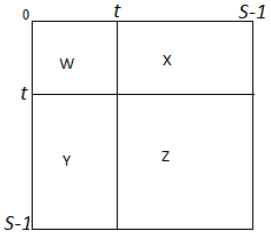

Figure 3 Partitioned co-occurrence matrix

Secondly, selecting the optimal threshold to classify foreground and background in the binarized image.

Writing the equations for following parameters:

$$P_W = \sum_{l=0}^{t}\sum_{k=0}^{t} P_{lk} \quad (8)$$

$$P_Y = \sum_{l=t+1}^{S-1}\sum_{k=t+1}^{S-1} P_{lk} \quad (9)$$

Normalization will result in the following equations for cell probabilities:

$$P_{lk}^{W} = \frac{p_{lk}}{P_W} = \frac{r_{lk}}{\sum_{l=0}^{t}\sum_{k=0}^{t} r_{lk}} \quad (10)$$

For $0 \le l \le t$, $0 \le k \le t$

Similarly

$$P_{lk}^{Y} = \frac{p_{lk}}{P_Y} = \frac{r_{lk}}{\sum_{l=t+1}^{S-1}\sum_{k=t+1}^{S-1} r_{lk}} \quad (11)$$

For $t+1 \le l \le S-1$, $t+1 \le k \le S-1$

March - April 2020
ISSN: 0193-4120 Page No. 12495 - 12505

Figure 4. Illustration of segmentation and post-processing on Filtered SODOG image: (a) Segmented image from modified entropy thresholding (b) Post-processed image after label filtering

The second order local entropy of the vessel and non-vessel is given by equations (12) and (13) respectively.

$$H_W^2(t) = -\frac{1}{2}\sum_{l=0}^{t}\sum_{k=0}^{t} p_{lk}^W \log_2 p_{lk}^W \quad (12)$$

$$H_Y^2(t) = -\frac{1}{2}\sum_{l=t+1}^{S-1}\sum_{k=t+1}^{S-1} p_{lk}^Y \log_2 p_{lk}^Y \quad (13)$$

Therefore, final second order modified local entropy is written as

$$H_T^2(t) = H_W^2(t) + H_Y^2(t) \quad (14)$$

The calculated $H_T^2(t)$ considered as threshold for vessel and non-vessel segmentation. Thresholding results for SODOG image of Fig. 2(b), is shown in Fig. 4(a) where it can be observed that retinal vascular tree is clearly detected.

D. Postprocessing

From Fig. 4(b), it can be observed that there are some wrongly classified pixels. Clear segmented image can be obtained by removing these isolated pixels. Here post-processing uses label filtering in order to eliminate the isolated pixels. The Label filtering tries to identify the isolated elements on 8-connected neighboring pixel propagation. After filtering, the resulting groups that exceeding for e.g., 200 pixels are considered as vessel pixels. Fig. 4(b) presents result of post-processing.

V. EXPERIMENT RESULTS

A. Performance Measures

Performance of the algorithm is quantified by comparing the final post-processed image with corresponding ground-truth image. Here, for the two filter based segmentation methods the following parameters, percentage of sensitivity (Se), percentage of specificity (Sp), percentage of accuracy (Acc), percentage of positive predictive value (Ppv) and percentage of Negative predictive value (Npv) are computed. These parameters are defined in Table I as

TABLE I CONTINGENCY CLASSIFICATION OF VESSELS

	Presence of Vessel pixel	**Absence of Vessel pixel**
Vessel pixel found	True positive fraction(TPF)	False positive fraction(FPF)
Vessel pixel not found	False negative fraction(FNF)	True negative fraction (TNF)

$$Se(\%) = \frac{TPF}{TPF + FNF} \times 100 \quad (15)$$

$$Sp(\%) = \frac{TNF}{TNF + FPF} \times 100 \quad (16)$$

$$Ppv(\%) = \frac{TPF}{TPF + FPF} \times 100 \quad (17)$$

$$Npv(\%) = \frac{TNF}{TNF + FNF} \times 100 \quad (18)$$

$$Acc(\%) = \frac{TPF + TNF}{TPF + FNF + TNF + FPF} \times 100 \quad (19)$$

Se and Sp parameters indicate measure of good classified vessels and background pixels respectively. Ppv is a measure of pixels categorized as vessel pixels that are rightly categorized. Npv is a measure of pixels categorized as non vessel pixels that is rightly categorized. And Acc is overall measure of total well-categorized pixels.The performance of the two filter based methods are also evaluated with receiver operating characteristic (ROC) curves, which is a plot of true positive fractions (Se) versus false positive fractions (1-Sp).

B. Proposed Method Evaluation

The performance results obtained from FODOG and SODOG on 20 images of STARE database is listed in Table II and III and of DRIVE database is listed in table IV and V. The tables show average Se, Sp, Ppv, Npv, and Acc values.

March - April 2020
ISSN: 0193-4120 Page No. 12495 - 12505

TABLE II PERFORMANCE OF FODOG ON IMAGES OF STARE DATASET

Sl. No	Se (%)	Sp (%)	Acc (%)	Ppv (%)	Npv (%)
Im-01	96.28	92.59	94.14	90.33	97.2
Im-02	98.32	**86.6**	**91.88**	**85.76**	98.43
Im-03	98.15	89.44	93.28	87.97	98.4
Im-04	95.22	97.8	96.79	96.54	96.94
Im-05	96.31	94.86	95.48	93.35	97.17
Im-06	98.46	93.31	95.66	92.52	98.64
Im-07	98.7	93.93	96.16	93.47	98.79
Im-08	**99.12**	94.02	96.45	93.77	**99.15**
Im-09	98.68	95.81	97.15	95.38	98.8
Im-10	97.78	96.41	97.03	95.67	98.17
Im-11	98.83	94.5	96.53	94.04	98.93
Im-12	98.82	96.57	97.63	96.23	98.93
Im-13	98.41	95.01	96.59	94.5	98.56
Im-14	98.55	94.85	96.58	94.41	98.67
Im-15	97.1	96.7	96.88	95.84	97.71
Im-16	94.51	97.15	96.06	95.87	**96.19**
Im-17	98.15	96.28	97.14	95.75	98.38
Im-18	98.27	**98.68**	**98.5**	**98.27**	98.68
Im-19	98.1	97.95	98.01	97.16	98.64
Im-20	97.53	94.98	96.08	93.63	98.07
Average	97.76	94.87	96.2	94.02	98.22

TABLE III PERFORMANCE RESULTS OF SODOG ON IMAGES OF STARE DATASET

Sl. No	Se (%)	Sp (%)	Acc (%)	Ppv (%)	Npv (%)
Im-01	96.11	92.49	93.99	90.08	97.1
Im-02	97.35	**90.89**	**93.64**	**88.82**	97.88
Im-03	98.46	91.59	94.67	90.52	98.64
Im-04	**94.04**	98.3	96.72	97.05	96.53
Im-05	96.39	96.04	96.19	94.83	97.25
Im-06	99.08	92.23	95.48	91.97	99.12
Im-07	98.7	93.93	96.16	93.47	98.79
Im-08	**99.12**	94.02	96.45	93.77	**99.15**
Im-09	98.68	95.81	97.15	95.38	98.8
Im-10	97.78	96.41	97.03	95.67	98.17
Im-11	98.83	94.5	96.53	94.04	98.93
Im-12	98.82	96.57	97.63	96.23	98.93

Im-13	98.41	95.01	96.59	94.5	98.56
Im-14	98.55	94.85	96.58	94.41	98.67
Im-15	97.1	96.7	96.88	95.84	97.71
Im-16	94.51	97.15	96.06	95.87	**96.19**
Im-17	98.15	96.28	97.14	95.75	98.38
Im-18	98.27	**98.68**	**98.5**	**98.27**	98.68
Im-19	98.1	97.95	98.01	97.16	98.64
Im-20	97.53	94.98	96.08	93.63	98.07
Average	97.7	95.22	96.37	94.36	98.21

TABLE IV PERFORMANCE OF FODOG ON IMAGES OF DRIVE DATASET

Sl. No	Se (%)	Sp (%)	Acc (%)	Ppv (%)	Npv (%)
Im-01	96.79	96.61	96.69	95.67	97.5
Im-02	95.48	97.49	96.63	96.56	96.68
Im-03	92.63	98.36	96.15	97.26	95.5
Im-04	93.58	98.62	96.66	97.74	96.02
Im-05	94.95	97.98	96.74	97.03	96.54
Im-06	**91.86**	**98.78**	96.19	**97.82**	**95.31**
Im-07	96.44	95.46	95.88	94.15	97.25
Im-08	93.83	96.76	95.63	94.78	96.15
Im-09	95.4	97.36	96.57	96.07	96.9
Im-10	94.72	97.95	96.67	96.77	96.61
Im-11	95.16	96.75	96.1	95.29	96.65
Im-12	94.26	97.89	96.47	96.65	96.36
Im-13	94.04	97.8	96.29	96.63	96.07
Im-14	97.2	95.93	96.48	94.87	97.79
Im-15	**98.26**	**92.88**	**95.32**	**91.96**	**98.48**
Im-16	95.56	96.64	96.19	95.29	96.83
Im-17	92.13	98.16	95.98	96.57	95.68
Im-18	94.35	98.13	96.67	96.92	96.53
Im-19	96.44	97.65	**97.14**	96.8	97.39
Im-20	94.79	98.11	96.84	96.9	96.8
Average	94.89	97.27	96.36	96.09	96.65

TABLE V PERFORMANCE OF SODOG ON IMAGES OF DRIVE DATASET

Sl. No	Se (%)	Sp (%)	Acc (%)	Ppv (%)	Npv (%)
Im-01	97.06	97.05	97.06	96.28	97.67
Im-02	96.74	97.52	97.17	96.89	97.4
Im-03	94.03	98.18	96.5	97.21	96.05

March - April 2020
ISSN: 0193-4120 Page No. 12495 - 12505

Im-04	95.82	98.24	97.22	97.54	96.99
Im-05	96.52	97.81	97.25	97.12	97.34
Im-06	95.76	97.43	96.72	96.5	96.88
Im-07	93.28	**98.64**	96.58	97.71	95.92
Im-08	**92.82**	97.62	**95.84**	95.85	**95.83**
Im-09	94.28	98.61	96.94	**97.71**	96.48
Im-10	97.69	96.02	96.76	95.21	98.09
Im-11	96.78	95.58	96.1	94.41	97.47
Im-12	97.15	96.56	96.82	95.69	97.73
Im-13	95.19	98	96.82	97.15	96.6
Im-14	97.33	96.92	97.1	96.11	97.89
Im-15	**98.21**	**95.11**	96.51	**94.3**	**98.47**
Im-16	95.24	98.01	96.87	97.09	96.72
Im-17	94.84	97.93	96.7	96.82	96.63
Im-18	94.52	98.39	96.89	97.38	96.6
Im-19	98.02	96.77	**97.34**	96.2	98.32
Im-20	96.08	97.99	97.21	97.05	97.32
Average	95.87	97.42	96.82	96.51	97.12

The ROC curves for DRIVE and STARE datasets using FODOG and SODOG filter methods is shown in Fig. 5 and Fig. 6.From the ROC curves it is observed that FODOG and SODOG methods give better performance with STARE database when compared to DRIVE database.

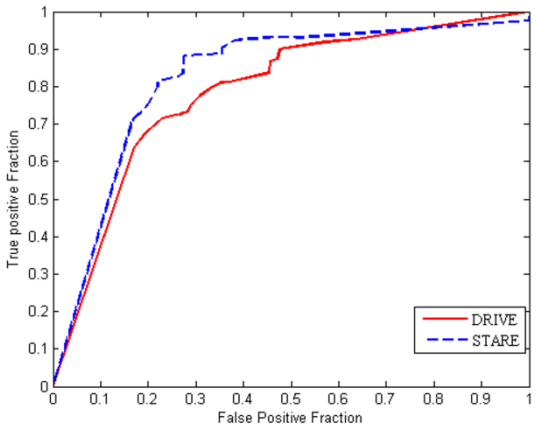

Figure 5. ROC curve for STARE and DRIVE databases using FODOG

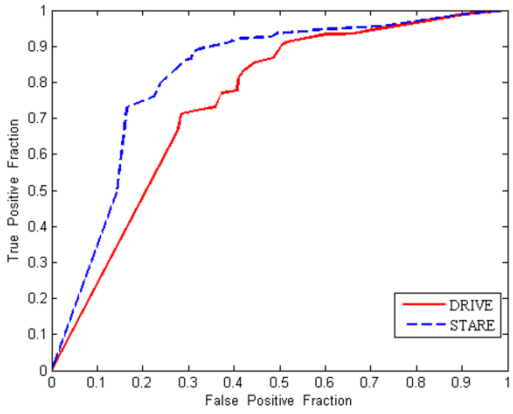

Figure *6. ROC curve for* STARE and DRIVE *databases using SODOG*

C .Comparison with Other Methods

Here our method is compared with the other retinal vessel segmentation algorithms. We used Acc value as a performance measuring parameter. Since other authors also have performed this type of measurement. This choice enables us to compare our results with theirs. Tables VI shows performance comparison results in terms of Acc, with the other published algorithms.

March - April 2020
ISSN: 0193-4120 Page No. 12495 - 12505

TABLE VI PERFORMANCE RESULTS COMPARED INTERMS OF AVERAGE ACCURACY WITH OTHER METHODS ON THE STARE AND DRIVE DATASETS

Method Type	Method	STARE	DRIVE	STARE + DRIVE
Supervised	Niemeijer *et al.* [8]	0.9417	-	-
	Staal *et al.* [9]	0.9441	-	-
	Soares *et al.* [10]	0.9466	0.948	0.9473
	Ricci and Perfetti [11]	0.9595	0.9646	0.9621
	Marin *et al* [12]	0.9452	0.9526	0.9489
Unsupervised	Chaudhuri *et al.* [20]	0.8773	-	-
	Hoover *et al.* [21]	-	0.9275	0.9471
	Mendonca *et al.* [25]	0.9463	0.9479	0.896
	Jiang *et al.* [26]	0.8911	0.9009	0.9377
	Martinez *et al.* [27]	0.9344	0.941	-
	Cinsdikici and Aydin [34]	0.9293	-	-
	This Work FODOG	0.962	0.9636	0.9628
	SODOG	**0.9637**	**0.9682**	**0.9659**

All the above segmentation techniques are explained in Section II. Values written in the table VI are reported by their authors for each dataset. The gaps in table indicate no calculation done for all 20 images. Last column in the table VI indicates overall average of accuracy on both the datasets.

From table VI it is clear that our FODOG method gives better Acc values compared to all other segmentation techniques on STARE images. But on DRIVE images our method is out performed by Ricci and Perfetti [11]. Our approach outperforms the result of Acc value achieved by all other authors when both databases are considered.

In case of SODOG method, our proposed algorithm clearly outperforms the Acc results of all other authors including our own FODOG technique on both STARE and DRIVE images and also it gives excellent Acc result when both the databases are considered.

VI. DISCUSSION AND CONCLUSION

Blood vessel segmentation and detection techniques reported in the literature are classified into supervised and unsupervised (Rule- based) methods. Our proposed method comes in unsupervised category. This algorithm uses Gaussian based filter technique. Here we used FODOG and SODOG filters followed by modified local entropy thresholding algorithm.

The proposed SODOG method results in highest Acc value on both the databases. Acc value obtained by our method is higher than that obtained by all other authors including our own FODOG method as reported in the table VI. And the Acc value reached by FODOG method is slightly higher than that of Mendonca *et al.* [25], Soares *et al.* [10], and Marin *et al.* [13]. Although Ricci and Perfetti [11] approach gives higher Acc value with DRIVE database. But in case of STARE it is outperformed by FODOG. Retinal vasculature segmentation tool should work effectively on images taken with different equipment. Our unsupervised algorithm works robustly on both the STARE and DRIVE databases when compared with other supervise methods.

March - April 2020
ISSN: 0193-4120 Page No. 12495 - 12505

In addition, supervised methods require more computation time of around 1 minute 30 seconds as reported by Marin *et al.* [12].On the other hand, our proposed method retains the computational simplicity and faster segmentations as it does not need training images as in case of supervised methods of classification. The time needed in processing each retinal image is less than 5 seconds, when run on a PC with an Intel Core i3CPU at 2.40GHz and 4 GB of RAM. And the method gives accurate segmentation results in the cases of normal as well as in obscure blood vessel retinal images. Even the smaller and tiny blood vessels can be detected.

The effectiveness and robustness of our algorithm, with simpleness and fast execution makes it an appropriate tool for automated analysis of retinal images and thereby aids in prescreening process for early DR detection.

ACKNOLWEDGMENT

We author's thank Prof. Chetan H CMR Institute of Technology providing technical support for continuing our research at the Embedded system center of excellence.

REFERENCES

[1] Ramandeep Singh, Kim Ramasamy, Chandran Abraham, Vishali Gupta, Amod Gupta, "Diabetic retinopathy: An update," Indian J Optholmol., vol. 56, No. 3, pp. 179-188, May-June 2008.

[2] S. Wild, G. Roglic, A. Green, R. Sicree, and H. King, "Global prevalence of diabetes: Estimates for the year 2000 and projections for 2030," Diabetes Care, vol. 27, pp. 1047–1053, 2004.

[3] E. J. Sussman, W. G. Tsiaras, and K. A. Soper, "Diagnosis of diabetic eye disease," J. Am. Med. Assoc., vol. 247, pp. 3231–3234, 1982.

[4] J.J Kanski, Clinical Opthalmology: A Systematic Approach. London, U.K.: Butterworth-Heinemann,1989.

[5] S. J. Lee, C. A. McCarty, H. R. Taylor, and J. E. Keeffe, "Costs of mobile screening for diabetic retinopathy: A practical framework for
rural populations," Aust. J. Rural Health, vol. 8, pp. 186–192, 2001.

[6] D. S. Fong, L. Aiello, T. W. Gardner, G. L. King, G. Blankenship, J. D. Cavallerano, F. L. Ferris, and R. Klein, "Diabetic retinopathy," Diabetes Care, vol. 26, pp. 226–229, 2003.

[7] H. R. Taylor and J. E. Keeffe, "World blindness: A 21st century perspective," Br. J. Ophthalmol., vol. 85, pp. 261–266, 2001.

[8] M. Niemeijer, J. Staal, B. v. Ginneken, M. Loog, and M. D. Abramoff, J. Fitzpatrick and M. Sonka, Eds., "Comparative study of retinal vessel segmentation methods on a new publicly available database," in SPIE Med. Imag., 2004, vol. 5370, pp. 648–656.

[9] J. Staal, M. D. Abràmoff, M. Niemeijer, M. A. Viergever, and B. v. Ginneken, "Ridge based vessel segmentation in color images of the retina," IEEE Trans. Med. Imag., vol. 23, no. 4, pp. 501–509, Apr. 2004.

[10] J. V. B. Soares, J. J. G. Leandro, R. M. Cesar, Jr., H. F. Jelinek, and M.J. Cree, "Retinal vessel segmentation using the 2D Gabor wavelet and supervised classification" IEEE Trans. Med. Image., vol. 25, no. 9, pp.1214–1222, Sep. 2006.

[11] E. Ricci and R. Perfetti, "Retinal blood vessel segmentation using line operators and support vector classification," IEEE Trans. Med. Imag., vol. 26, no. 10, pp. 1357–1365, Oct. 2007.

[12] Diego Marín, Arturo Aquino, Manuel Emilio Gegúndez- Arias, and José Manuel Bravo, "A New Supervised Method for Blood Vessel Segmentation in Retinal Images by Using Gray-Level and Moment Invariants-Based Features" IEEE Trans. On medical imaging, vol.30, NO. 1-Jan-2011.

[13] I. Liu and Y. Sun, "Recursive tracking of vascular networks in angiograms based on the detection-deletion scheme," IEEE Trans. Med. Imag., vol. 12, no. 2, pp. 334–341, Jun. 1993.

[14] L. Zhou, M. S. Rzeszotarski, L. J. Singerman, and J. M. Chokreff, "The detection and quantification of retinopathy using digital angiograms," IEEE Trans. Med. Imag., vol. 13, no. 4, pp. 619–626, Dec. 1994.

[15] O. Chutatape, L. Zheng, and S. M. Krishnan, "Retinal blood vessel detection and tracking by matched Gaussian and Kalman filters," in Proc. 20th Annu. Int. Conf. IEEE Eng. Med. Biol. Soc. (EMBS'98), 1998, vol. 20, pp. 3144–3149.

[16] Y. A. Tolias and S. M. Panas, "A fuzzy vessel tracking algorithm for retinal images based on fuzzy clustering," IEEE Trans. Med. Imag., vol. 17, no. 2, pp. 263–273, Apr. 1998.

[17] A. Can, H. Shen, J. N. Turner, H. L. Tanenbaum, and B. Roysam, "Rapid automated tracing and feature extraction from retinal fundus images using direct exploratory algorithms," IEEE Trans. Inf. Technol. Biomed., vol. 3, no. 2, pp. 125–138, Jun. 1999.

March - April 2020
ISSN: 0193-4120 Page No. 12495 - 12505

[18] M. Lalonde, L. Gagnon, and M.-C. Boucher, "Non-recursive paired tracking for vessel extraction from retinal images," Vision Interface, pp. 61–68, 2000.

[19] X. Gao, A. Bharath, A. Stanton, A. Hughes, N. Chapman, and S. Thom, "A method of vessel tracking for vessel diameter measurement on retinal images," in Proc. ICIP'01, 2001, pp. II: 881–884.

[20] S. Chaudhuri, S. Chatterjee, N. Katz, M. Nelson, and M. Goldbaum, Detection of blood vessels in retinal images using two dimensional matched filters, IEEE Trans. Medical imaging, vol. 8, no. 3, September 1989.

A. Hoover, V. Kouznetsova and M. Goldbaum, "Locating blood vessels in retinal images by piecewise threshold probing of a matched filterresponse", IEEE Trans. Med. Imag., vol. 19, no. 3, pp. 203-210, 2000.

[21] Chanwimaluang, Thitiporn Sch. of Electr. & C omput. Eng., Oklahoma State Univ., Stillwater, OK, USA Fan, Guoliang L., "An efficient blood vessel detection algorithm for retinal images using local entropy thresholding", IEEE trans. Circuits and Systems, 2003. ISC AS '03. Proceedings of the, Volume: 5 Page(s): V-21 - V-24, 2003.

[22] F. Zana and J. C. Klein, "Segmentation of vessel-like patterns using mathematical morphology and curvature evaluation," IEEE Trans. Image Process., vol. 10, no. 7, pp. 1010–1019, Jul. 2001.

[23] B. Fang, W. Hsu, and M. Lee, "Reconstruction of vascular structures in retinal images," in Proc. ICIP'03, 2003, pp. II: 157–160

[24] A. M. Mendonça and A. Campilho, "Segmentation of retinal blood vessels by combining the detection of centerlines and morphological reconstruction," IEEE Trans. Med. Imag., vol. 25, no. 9, pp. 1200–1213, Sep. 2006.

[25] X. Jiang and D. Mojon, "Adaptive local thresholding by verificationbased multithreshold probing with application to vessel detection in retinal images," IEEE Trans. Pattern Anal. Mach. Intell., vol. 25, no. 1, pp. 131–137, Jan. 2003.

[26] M. E. Martinez-Perez, A. D. Hughes, S. A. Thom, A. A. Bharath, and K. H. Parker, "Segmentation of blood vessels from red-free and fluorescein retinal images," Med. Imag. Anal., vol. 11, pp. 47–61, 2007.

[27] Onkaew, D, "Automatic extraction of retinal vessels based on gradient orientation Analysis," IEEE Trans. Computer Science and Software Engineering (JC SSE), 2011 Page(s): 102 – 107.

[28] L. Streeter and M. J. Cree, "Microaneurysm detection in colour fundus images," in Image Vision Comput. New Zealand, Palmerston North, New Zealand, Nov. 2003, pp. 280–284.

[29] M. Niemeijer, B. van Ginneken, J. J. Staal, M. S. A. Suttorp-Schulten,and M. D. Abramoff, "Automatic detection of red lesions in digital color fundus photographs," IEEE Trans. Med. Imag., vol. 24, no. 5, pp. 584–592, May 2005..

[30] T. Walter, P. Massin, A. Erginay, R. Ordonez, C. Jeulin, and J. C. Klein,"Automatic detection of microaneurysms in color fundus images," Med. Image Anal., vol. 11, pp. 555–566, 2007.

[31] Research Section, Digital Retinal Image for Vessel Extraction (DRIVE) Database. Utrecht, The Netherlands, Univ. Med. Center Utrecht, Image Sci. inst. [online]. Available: http://www.isi.uu.nl/Re-search/Databases/

[32] STARE ProjectWebsite. Clemson, SC, Clemson Univ. [Online]. Available: http://www.ces.clemson.edu/

[33] M. G. Cinsdikici and D. Aydin, "Detection of blood vessels in ophthalmoscope images using MF/ant (matched filter/ant colony) algorithm," Comput. Methods Programs Biomed., vol. 96, pp. 85–95, 2009.

[34] Jianqiang Lia, Qidong Hua, Azhar Imrana, Li Zhangb, Ji-jiang Yangc, Qing Wangc, "Vessel Recognition of Retinal Fundus Images Based on Fully Convolutional Network", 42nd IEEE International Conference on Computer Software & Applications, vol. 2, July 2018.

First author

Manjunath V Gudur received the B.E in Electronics and Communication Engineering from the Visvesvaraya Technological University, Belgaum, in 2011. He received his Master of Technology in Biomedical Signal Processing and Instrumentation from SJCE, Mysuru, India in 2013.

Presently he is working as a Assistant Professor in the Department of Electronics and Communication Engineering, CMR Institute of Technology Bengaluru, Karnataka, India. His research interests include Medical Image Processing, Digital Signal and Image Processing, Pattern Recognition, Analog and Digital Communications.